

Contrails, Cirrus Trends, and Climate

Patrick Minnis,

Atmospheric Sciences
NASA Langley Research Center
Hampton, Virginia USA

J. Kirk Ayers, Rabindra Palikonda, and Dung Phan

Analytical Services and Materials, Inc.
Hampton, Virginia USA

Submitted to *Journal of Climate*, July 2003

Abstract

Rising global air traffic and its associated contrails have the potential for affecting climate via radiative forcing. Current estimates of contrail climate effects are based on coverage by linear contrails that do not account for spreading and, therefore, represent the minimum impact. The maximum radiative impact is estimated by assuming that long-term trends in cirrus coverage are due entirely to air traffic in areas where humidity is relatively constant. Surface observations from 1971-1995 show that cirrus increased significantly over the northern oceans and United States of America (USA) while decreasing over other land areas except over western Europe where cirrus coverage was relatively constant. The surface observations are consistent with satellite-derived trends over most areas. Land cirrus trends are positively correlated with upper tropospheric (300 hPa) humidity (UTH), derived from National Center for Environmental Prediction (NCEP) analyses, except over the USA and western Europe where air traffic is heaviest. Over oceans, the cirrus trends are negatively correlated with the NCEP relative humidity suggesting some large uncertainties in the maritime UTH. The NCEP UTH decreased dramatically over Europe while remaining relatively steady over the USA, thereby permitting an assessment of the cirrus-contrail relationship over the USA. Seasonal cirrus changes over the USA are generally consistent with the annual cycle of contrail coverage and frequency lending additional evidence of the role of contrails in the observed trend. The cirrus increase is a factor of 1.8 greater than that expected from current estimates of linear contrail coverage suggesting a spreading factor of the same magnitude can be used to estimate the maximum effect of the contrails. From the USA results and using a mean contrail optical depth of 0.15, the maximum contrail-cirrus global radiative forcing is

estimated to be $0.006 - 0.015 \text{ Wm}^{-2}$ depending on the radiative forcing model. The greater value is slightly less than that for the earlier “best estimate” for linear contrails because of the reduced optical depth. It is concluded that the USA cirrus trends are most likely due to air traffic. Additionally, the seasonal cirrus trends over the USA can account for much of the observed warming between 1975 and 1994.

1. Introduction

Condensation trails, or contrails, generated from high-altitude aircraft exhaust may affect climate because they can persist for many hours. Like their natural counterparts, these anthropogenic cirrus clouds reflect solar radiation and absorb and emit thermal infrared radiation causing a radiative forcing that depends on many factors especially contrail optical depth and coverage (Sassen, 1997; Meerkötter et al. 1999). Cloud radiative forcings are balanced by changes in variables such as surface and atmospheric temperatures, cloud cover, and precipitation (Hansen et al. 1997). Instantaneously, contrail radiative forcing can warm the atmosphere and warm or cool the Earth's surface, apparently reducing the diurnal range of surface temperature (Travis et al. 2002). Although highly variable and uncertain, this forcing is generally positive when averaged over time (Minnis et al. 1999; Ponater et al. 2002; Meyer et al. 2002), resulting in a net warming of the troposphere and surface (Rind et al. 2000). The expected 2 – 5% per annum growth (IPCC, 1999) of worldwide jet air traffic through 2050 necessitates a more accurate assessment of contrail climate effects.

Current estimates of contrail radiative forcing only consider linear contrails young enough to be differentiated from natural cirrus clouds in satellite images. Those diagnoses of radiative forcing represent the minimum impact because they do not include the additional cloud cover resulting from the spread of aging linear contrails into natural-looking cirrus clouds (Minnis et al. 1998; Duda et al. 2001) and from any other cirrus clouds initiated by aerosols generated from aircraft exhaust (Jensen and Toon, 1994). To reduce the uncertainty in the climatic effects of aircraft-induced cirrus clouds, it is necessary to determine the maximum change in cirrus coverage due to the combination of

linear contrails and the cirrus clouds derived from them and from exhaust aerosols (IPCC, 1999). The ratio of that combination to the linear contrail coverage is denoted as the spreading factor f_s .

Increases in cirrus coverage or decreased sunshine have been linked to jet air traffic over parts of the contiguous USA (Changnon et al. 1981; Sassen, 1997) and Alaska (Nakanishi et al. 2001) for many years. Trends in regional cirrus frequency of occurrence are strongly correlated with high-altitude airplane fuel consumption between 1982 and 1991 (Boucher, 1999). Previous studies confirm the expected outcome of increased air traffic, but are limited to small regions or to time periods too short for minimizing the impact of the 11-year cycle in cloud cover (Udelhofen and Cess, 2001). In this study, a 25-year surface observation dataset is used to examine the longer term global trends in cirrus amounts, relate them to the expected contrail coverage to estimate f_s , and then compute the maximum regional contrail-induced radiative forcing and regional temperature changes.

2. Background

Contrails occupy a fairly special niche in atmospheric thermodynamics because they produce ice clouds at supersaturations below the relative humidities required for most natural cirrus cloud formation (Gierens et al. 1999). The presence of cirrus or persistent contrails depends on many factors such as temperature T , humidity, vertical velocity, and cloud condensation and freezing nuclei. The primary variable, however, is relative humidity. The complex dynamical processes initiating cirrus formation ultimately must produce the necessary water vapor. The most familiar moisture variable, relative

humidity with respect to liquid water (Rh), is measured with radiosonde-borne hygrometers and used in weather analyses. For cirrus processes, the relative humidity with respect to ice (Rhi) is the relevant quantity. It exceeds Rh for a given specific humidity at $T < 0^\circ\text{C}$. Cirrus clouds form naturally through heterogeneous or homogeneous nucleation at low temperatures when the ambient Rhi is around 140-160% (Sassen and Dodd, 1989), but will persist as long as Rhi exceeds 100%. Contrails can form and develop into cirrus clouds when $T < -39^\circ\text{C}$ and $Rhi > 100\%$ because, in many instances, aircraft exhaust temporarily raises the local Rh above 100% causing nucleation of liquid droplets that freeze instantly. For $T < -39^\circ\text{C}$, $Rh > 100\%$ typically corresponds to $Rhi > 150\%$. Therefore, contrails can add to the natural cirrus coverage when $T < -39^\circ\text{C}$ and $100\% < Rhi < 150\%$ and no natural cirrus cloud is already present (Fig. 1).

At flight altitudes, conditions that can support contrail-generated cirrus clouds exist 10 - 20% of the time in clear air and within existing cirrus (Gierens et al. 1999; Jensen et al. 2001). Additionally, cirrus may form at lower supersaturations from aerosols derived from jet aircraft (Jensen and Toon, 1994). Therefore, high-altitude air traffic has the potential for increasing cirrus coverage and thickening existing cirrus clouds by generating additional ice crystals without directly diminishing the potential for natural cirrus development. If other relevant variables are steady over time, then cirrus coverage should increase where air traffic is significant.

3. Data

The surface-based cloud data consist of quality-controlled surface synoptic weather reports from land stations and ships filtered by Hahn and Warren (1999). Reports from

automated weather stations and those with obvious errors and inconsistencies were eliminated from the dataset. The observations include cloud type frequency of occurrence and amount-when-present (AWP) as well as total cloud amount. The cirrus amount for a given observation is found by multiplying AWP by frequency of occurrence, a computation that implicitly assumes that the clouds are randomly overlapped. Annual and seasonal mean cirrus and total cloud amounts were calculated over land and ocean regions between 1971 and 1995. Although the original surface-based cloud dataset includes 1996, the number of surface stations in the United States declined dramatically after 1995 affecting the sampling patterns. Data from multiple stations within a single grid-box for a given month were averaged first for each site and then with the means from the other stations to yield a monthly grid box average. Annual means for land were calculated for 3° grid-boxes having a minimum of 60 valid observations, 10 valid upper level cloud observations, and a minimum of 15 years of data. Annual means for ocean were calculated for 5° grid-boxes having a minimum of 30 valid observations, 5 valid upper level clouds observations and minimum of 7 months of data per year. Only data taken between 70°N and 60°S were used in the calculation of averages for the air traffic regions (ATRs) that are defined in Table 1.

Monthly mean cirrus and cirrostratus fractions from the International Satellite Cloud Climatology Project (ISCCP; Rossow and Schiffer, 1999) D2 dataset were combined to provide cirrus coverage on a 250 x 250 km² grid for 1984 – 1996 as a consistency check on the surface observations. Only data taken between July 1983 and June 1991 and between July 1993 and June 1996 were used here to minimize the impact of the Mt. Pinatubo eruption on the satellite retrievals. Values from ISCCP categories of cirrus and

cirrostratus were summed to provide estimates of total cirrus coverage. Only daytime amounts were used for high clouds. The ISCCP ATR averages were computed using only the same grid boxes that were included in the surface ATR analyses.

Annual mean relative humidities (RH) with respect to liquid water at 300 hPa ($RH3$) computed on a 2.5° grid from the National Center for Environmental Prediction reanalyses (NCEP) are used to evaluate the changes in upper tropospheric humidity (UTH) that can affect cirrus variability (Kistler et al. 2001). The mean annual distribution of expected linear contrail coverage ($ECON$) on a 2.8° grid is based on a combination of satellite observations, air traffic data from 1992, and a parameterization of contrail formation applied to 10 years of global numerical weather analyses (Sausen et al. 1998). The air traffic data are based on the assumption of great circle routes between two airports.

4. Results and discussion

a. Cirrus Trends

Linear trends, $\Delta CC / \Delta t$, in annual mean cirrus coverage (CC) with time, t , were computed for each grid box having averages for more than 15 years. CC increased over the USA, the north Atlantic and Pacific, and Japan (Fig. 2a), but dropped over most of Asia, Europe, Africa, and South America. Increases are also evident around coastal Australia, sub-Saharan western Africa, and over the South Atlantic west of Africa. Areas with no trends were insufficiently sampled. Many of the trends are statistically significant at the 90% confidence level (Fig. 2b). The largest concentrated increases occurred over the northern Pacific and Atlantic and roughly correspond to the major air traffic routes

reflected in the *ECON* distribution (Fig. 2c). Increased *CC* over the USA and around Australia and Japan coincide with relatively well-traveled routes. Over Europe, the *CC* trends are mixed, while $\Delta CC/\Delta t$ is negative over South American routes. The coincident NCEP *RH3* dropped dramatically over Europe and northeastern Asia and less so over the northeastern USA, much of Asia, and the temperate ocean regions (Fig. 2d). *RH3* rose over much of the Tropics, northern China, and southwestern USA and adjacent waters.

Although there appears to be close correspondence between many air traffic routes and increased *CC*, some differences exist between the local maxima in $\Delta CC/\Delta t$ and *ECON*. Assuming that contrails caused the changes in *CC*, then such differences could arise from slight discrepancies in gridding, idealization of air routes, and contrail movement. Contrails often advect hundreds of kilometers as they develop. Thus, their region of origin may differ from the area with maximum change in *CC*. To reduce this regional noise, the data were grouped into larger areas of contrail influence. The boxes in Fig. 2c show the ATRs while the remaining areas constitute the other-region (OR) categories (see Table 1). The western European region (WEUR) is a subset of the European region (EUR). If contrails induce more cirrus coverage, then the largest effects should occur over the USA and WEUR where *ECON* is greatest (Table 2).

The yearly ATR *CC* averages (Fig. 3) rose over the USA, remained steady over WEUR, and decreased over EUR, western Asia and the land OR (LOR). *CC* also increased over the North Pacific (NP) and North Atlantic (NA) as well as over the ocean OR (OOR). Interannual variability in *CC* (Table 2) is greatest over Europe and least over the LOR. Trends in *CC* are mostly of the same sign as the total cloud cover trends (Table 2) and can account for most of the total cloud cover change over Asia, the LOR, and the

NP. The increase in CC over the USA is compensated by slight decreases in other cloud types, while the opposite is true for EUR. Because CC is based on the assumption of random overlap, i.e., $CC = Ci(1 + OC)$, the total cloud coverage is

$$TC = Ci + OC, \quad (1)$$

where OC is other cloud coverage and Ci is the actual observed cirrus coverage. Using the original annual means of CC and TC for the USA, it can be shown that OC decreased by only 0.65% between 1971 and 1995, while Ci rose from 20.1% to 21.9%. Thus, the trend in OC is only -0.3%/dec. Over WEUR, the 0.7%/dec drop in total cloudiness is likely due to a decrease in low and mid-level cloud cover because CC remained constant. Total cloudiness increased more than CC over the OOR while $\Delta CC/\Delta t$ over the NA appears to have been compensated by decreases in other clouds.

The growth in ISCCP cirrus coverage over the USA greatly exceeds that from the surface observations (Table 2). Conversely, the ISCCP cirrus changes over the LOR and WEUR are less than half of those in CC . Except over the NA, the ISCCP ocean cirrus trends are small compared to those from the surface data. Discrepancies between the two trends are expected given the differences in sampling and observation techniques. Over the NP, $\Delta CC/\Delta t$ is positive but the ISCCP trend is negative, perhaps reflecting the difficulty in detecting cirrus from the visible and infrared satellite data when low clouds are prevalent underneath the cirrus. From atlases of cloud co-occurrence (Warren et al. 1986, 1988), it was found that the chance of cirrus occurring over stratus, midlevel clouds and nimbostratus is 20-40% more likely over the NP than over the NA. Additionally,

cirrus occurs without any other clouds present nearly twice as often over the NA than over the NP. Conversely, cirrus occurs 20% more often over cumulus clouds, which have large areas of clear between them, in the NA than in the NP. Thus, any trends in cirrus coverage detected over the NP with the ISCCP data are likely to be diminished in magnitude relative to those over the NA. The surface observations account for the overlap effects by applying a random overlap correction, but do not misclassify cirrus as some other cloud type. Except for the NP case, the sign of $\Delta CC/\Delta t$ is consistent with the ISCCP trends for the period common to both suggesting that the trends are not artifacts of the observation methods.

The frequency of clear-sky observations was also computed for the land ATRs. Over the USA and Asia, the frequency of clear skies changed by -1.3 and 1.8%/dec, respectively. Over Europe and WEUR, clear-sky frequency decreased by 0.6 and 0.7%/dec, respectively. Thus, over the USA, the increase in cirrus coverage was accompanied by fewer totally clear skies indicating that both the amount and frequency of cirrus coverage increased during the period.

Seasonal CC trends over the USA (Fig. 4a) are generally consistent with the seasonal variations of contrail occurrence frequency (Minnis et al. 2003), satellite contrail coverage (Palikonda et al. 1999, 2002) and $ECON$. The greater spring and winter trends are accompanied by maxima in contrail frequency and coverage while all three quantities dip during summer. Over WEUR, $\Delta CC/\Delta t$ averaged 1.0%/dec during summer and fall and -1.0%/dec during winter and spring (Fig. 4b), a seasonal variation differing from the satellite-based contrail coverage (Meyer et al. (2002) and $ECON$. Over western Asia, EUR, and the LOR, $\Delta CC/\Delta t$ was negative during all seasons except for summer over

Asia. Maximum $\Delta CC/\Delta t$ occurred during spring, summer, and fall over the NA, NP, and OOR, respectively.

b. Humidity impact

Most contrails form between 200 and 300 hPa where often $T < -39^\circ\text{C}$. The lowest pressure, p , with Rh reported in the NCEP reanalyses is 300 hPa. When $Rhi = 100\%$, the minimum threshold for cirrus and contrail formation, Rh should be about 68% at -40°C and 60% at -50°C (Fig. 1). Given the known biases and uncertainties in radiosonde Rh measurements at low temperatures (Sassen, 1997; Miloshevich et al. 2001), a more conservative estimate of the formation threshold would be 40% at -40°C , and less at lower temperatures. Thus, persistent contrails are likely to form if $Rh > 40\%$ and $T < -39^\circ\text{C}$ as measured from radiosondes, while cirrus clouds are more likely to form at a higher Rh threshold (Ponater et al. 2002). The correlations in Fig. 5 of $RH3$ with the annual frequency of $Rh(300 \text{ hPa}) > 40\%$ from radiosonde data at 78 locations in the Comprehensive Aerological Research Data Set (CARDS; see Eskridge et al. 1995) shows that $RH3$ is an excellent predictor of the frequency of humidity levels conducive to contrail and cirrus formation at 300 hPa. Comparisons with radiosonde data (Minnis et al. 2003) show that $RH3$ is highly correlated with the frequencies of $Rh(250 \text{ hPa})$ and $Rh(200 \text{ hPa})$ greater than 40%, having squared linear correlation coefficients R^2 of 0.74 and 0.52, respectively. Thus, $RH3$ can be used as a measure of the long-term variations in the frequency of persistent contrail conditions within the typical contrail altitude range.

Radiosondes at a given location may give accurate profiles of Rh instantaneously, but are subject to considerable error in the long term because of instrument changes and

variations in reporting practices (Elliot and Gaffen, 1991; Gaffen, 1993). Over land, NCEP incorporates radiosonde data, adjusting the profiles when necessary to maintain consistency with the model physics (Kistler et al. 2001). Over oceans, only radiosonde data from islands and coastlines are assimilated by NCEP; no other maritime humidity data are used. Comparisons of NCEP *RH3* values with those from other sources yield mixed results, but CARDS and NCEP are positively correlated over land at some level of significance, except over the USA (see Appendix). NCEP and CARDS are most consistent over Europe where the negative *RH3* trend (Fig. 2d) is strongest. The NCEP data used here are currently the best available estimate of UTH over land for the study period (see Appendix).

Trends in *RH3*, $\Delta RH3 / \Delta t$, are negative everywhere except over the USA (Table 3), where the trend is insignificant. Mean temperatures at 300 hPa are below -39°C everywhere except over the OOR (Table 3). Figure 6 shows scatterplots of and linear regression fits to *RH3* and *CC* data over the land regions. The lack of a *RH3-CC* correlation over the USA (Fig. 6c) and WEUR (Fig. 6b) indicates that the cirrus variation cannot be explained by the NCEP UTH trends. However, *RH3* explains 39%, 46%, and 33% of the variance in *CC* over Western Asia (Fig. 6a), EUR (Fig. 6b), and the LOR (Fig. 6d), respectively, where *ECON* is relatively small. The slopes of the respective linear fits (Fig. 6) are 0.3, 0.2, and 0.6 %*CC* / %*RH3*, suggesting that *CC* is less sensitive to changes in *RH3* over EUR, where *ECON* is relatively large, than over the LOR. Over ocean, *CC* and *RH3* are negatively correlated with R^2 ranging from 0.30 to 0.39 highlighting the poor quality of UTH over the oceans. Hereafter, only humidity impacts over land are considered.

The trend in total cirrus coverage CC can be estimated as the sum of the trend in contrail-cirrus and the dependence of natural cirrus coverage $cnat$ on $RH3$,

$$\frac{\partial CC}{\partial t} = \frac{\partial cnat}{\partial RH3} \frac{\partial RH3}{\partial t} + \frac{\partial ECON}{\partial t} f_s. \quad (2)$$

where $\partial ECON/\partial t$ is estimated from $ECON$ (Table 2) and the growth in air traffic ($ECON$ is assumed to be zero in 1970 for Asia and the LOR). CC increased over the USA despite no change in $RH3$, while it remained relatively steady over WEUR as $RH3$ plummeted. Between 1970 and 1995, air traffic increased by factors of 3.7 and 5.2 over the USA and Europe (IPCC, 1999), respectively, augmenting the respective contrail-forming potentials by approximately 15 and 21% each year relative to 1970 air traffic. If the frequency distribution of Rh remained steady throughout the period, then CC should have increased over those regions. Additional air traffic each year would produce more contrail-cirrus for $100\% < Rhi < 140\%$ (Area B in Fig. 1) while natural cirrus coverage would remain constant, resulting in a net increase in CC as seen for the USA. If the frequency of $Rh > 40\%$ decreased each year as indicated by $RH3$, then natural cirrus coverage would decrease proportionately as seen for the LOR, EUR, and Asia. A simultaneous rise in air traffic would produce proportionately more contrail-cirrus for $100\% < Rhi < 140\%$. In that instance, CC should decrease at a smaller rate than expected for aircraft-free conditions. The amount of counterbalancing would depend on the absolute annual increase in flights and the reduction rate in $RH3$. Over WEUR, the greater number of flights is apparently sufficient to offset the decrease in $RH3$, while over western Asia and the LOR, the smaller amount of air traffic would have less impact and is probably

insufficient to offset the drop in $RH3$. Large interannual changes in $RH3$ can affect the occurrence of both cirrus and contrails (Minnis et al. 2003), but over the long term, increases in air traffic should offset some of the reduction in CC caused by decreases in $RH3$.

Assuming that $ECON$ increased linearly with air traffic, the correlation between $ECON$ and CC is negative over the LOR, Western Asia, and EUR and near zero over WEUR. A fit to the USA data for $ECON$ increasing by 15%/y relative to 1971 yields $R^2 = 0.42$. This degree of correlation is comparable to that between $RH3$ and CC over LOR and EUR. Thus, over the one ATR where $RH3$ appears to be essentially invariant, air traffic can account for changes in CC as well as $RH3$ can in the ATRs where $RH3$ changes significantly. Over WEUR, a two-parameter fit using $RH3$ and $ECON$ to predict CC yields a negligible increase (0.0006 to 0.014) in R^2 relative to the correlation in Fig. 6b suggesting that the interannual variability is too large or the dramatic decrease in $RH3$ during the period had an inordinate impact on the frequency distributions of Rhi .

Any conclusion about the role of aircraft in the USA CC trends must consider all of the evidence rather than the humidity trends alone because of the uncertainties in $RH3$. Prior to 1994, few measurements were taken over the USA when $T < -40^\circ\text{C}$. However, CC and $RH3$ are also uncorrelated over WEUR, where $RH3$ is consistent with both satellite and radiosonde observations (see Appendix) and $ECON$ is comparable to that over the USA. This similarity supports the absence of an $RH3$ trend over the USA. The seasonal variations in the USA CC trends from both surface and satellite data have the same general characteristics as the magnitudes of the trends in contrail coverage. No statistically significant seasonal trends were found in $RH3$ over the USA, further

suggesting that relative humidity is not responsible for the *CC* trends. Given the positive *CC* trends in the surface and satellite observations, the seasonal consistency between contrails and $\Delta CC/\Delta t$, the lack of an *RH3* trend, an increase in cirrus frequency, and the known impacts of contrails on cirrus coverage, it is concluded that air traffic is most likely responsible for the 1%/dec growth in *CC* over the USA. It appears that cirrus coverage would have diminished over WEUR without the continually increasing high-altitude air traffic. In a similar vein, *CC* probably would have decreased more over western Asia, the remainder of Europe, and the LOR without contrails. Air traffic probably contributed to the increase of *CC* over the studied ocean areas. However, without improved estimates of UTH over the ocean, it will be difficult to determine the magnitude of that impact.

Based on the air traffic increase, the estimated linear contrail coverage rose by 0.55%/dec over the USA compared to the 1%/dec growth rate in *CC*. Assuming that the remaining *CC* increase is due to spreading contrails not detected by satellite analysis, $f_s = 1.8$. If the USA case is representative, the maximum impact of linear contrails plus the extra contrail-induced cirrus clouds should be roughly twice that determined for *ECON*. If the *ECON* values differ from the actual linear contrail coverage as derived from satellites, then f_s would change accordingly. Assuming that $f_s = 1.8$ for all land areas, the change of natural cirrus with the change in *RH3* over EUR, Asia, and the LOR is estimated to be 0.3, 0.3, and 1.4%/RH3, respectively. The value for the USA cannot be determined because *RH3* was invariant.

c. Climate effects

As of 1999, the “best” estimate of maximum net global radiative forcing, $FNET = 0.017 \text{ Wm}^{-2}$, at the top of the atmosphere computed for *ECON* was based on a contrail optical depth τ of 0.3 and the occurrence of contrails only at a pressure level of 200 hPa (Minnis et al. 1999). Recent studies by Ponater et al. (2002), Meyer et al. (2002), and Duda et al. (2003) indicate that, on average, τ is closer to 0.15 and the mean contrail pressure is closer to 225 hPa. Assuming that $\tau = 0.15$ and retaining the contrail pressure of 200 hPa, the maximum value of $FNET$ including both linear contrails and the resulting contrail-generated cirrus clouds would be 0.0153 Wm^{-2} because f_s would almost compensate for the reduction in τ . Increasing the pressure to 225 hPa would reduce the estimate slightly because the temperature difference between the two levels is approximately 3.5 K. The minimum global estimate of $FNET$ for linear contrails (Marquart and Mayer, 2002) is 0.0032 Wm^{-2} , a value that would almost double if f_s is considered. Thus, for the combination of contrails and aged-contrail cirrus coverage, the maximum global $FNET$ for 1992 air traffic is most likely between 0.006 and 0.015 Wm^{-2} yielding an overall range of 0.003 to 0.015 Wm^{-2} in radiative forcing by aircraft-induced cirrus clouds.

The immediate response to $FNET$ is warming of the atmosphere below the contrail and cooling or warming of the surface depending on the time of day (Meerkötter et al., 1998). Long-term responses to aircraft-induced cirrus have been estimated by inserting small percentages of cirrus into a general circulation model (GCM) at various time steps along the air traffic routes and then running the model to equilibrium (Rind et al. 1999). For a 1% change in absolute cirrus coverage with $\tau = 0.33$, the GCM yielded surface

temperature changes (ΔT_s) of 0.43°C and 0.58°C over the globe and Northern Hemisphere, respectively. The GCM mean tropospheric temperature between 3 and 10 km, ΔT_a , rose by $\sim 0.78^\circ\text{C}$. The regional variation in $\Delta CC/\Delta t$ (Table 3) and in the $RH3$ trends would prevent a direct application of the GCM results to estimate the global temperature impact of contrail-induced CC changes. Estimation of the temperature impact of $\Delta CC/\Delta t$ is more straightforward over the USA because the UTH is relatively steady and the CC trend accounts for most of the total cloudiness trend.

The estimation of the contrail-cirrus effect on the surface and tropospheric temperatures over the USA uses the Rind et al. (1999) values of ΔT_s for the Northern Hemisphere and ΔT_a for the globe. The latter value was used because it was the only tropospheric value available. The temperature trends were computed for the cirrus cover changes as follows:

$$\Delta T/\Delta t = 0.15/0.33 \Delta T D \Delta CC/\Delta t, \quad (3)$$

where ΔT is either the surface or tropospheric temperature change for each percent cirrus coverage, the ratio of $0.15/0.33$ accounts for the differences in contrail optical depth used here and by Rind et al. (1999), and D is the diurnal correction factor. The GCM study did not include the diurnal variation of contrail coverage, which is considerably reduced between 0000 and 0600 local time over the USA. The GCM also inserted the simulated contrails during clear-sky conditions. The traffic during the night is roughly half that during the day. Assuming that the unit nighttime forcing over land is 90% of that during the day due to heating and cooling of the surface and using the results for $\beta = 0.3$ in Table

1 from Minnis et al. (1999), the total longwave forcing computed in the absence of a diurnal cycle in air traffic would be 31% greater than that for a day-night ratio of 2. The net forcing for the diurnal ratio case would be 32% smaller than that for the no-diurnal case. Thus, D would be 0.68. However, Minnis et al. (1999) accounted for cloud overlap, which tends to reduce the shortwave forcing more than it reduces the longwave forcing. Thus, D should be slightly greater. A value of $D = 0.75$ is used here to account for the compensating affects not included in the GCM study. The true value of D is probably somewhere between 0.68 and 0.80. The actual response to increased CC via contrails is not likely to be in equilibrium because of the sporadic nature of contrail outbreaks and the steadily increasing air traffic. The instantaneous response, which can be much larger than the equilibrium value, would also not be appropriate because of the long time period considered and the tendency of significant contrails to last many hours and occur at different times of day. Thus, a slightly larger value of temperature response to changes in CC may be more appropriate and the values used are probably a conservative estimate. From (3), the respective surface and air temperature trends are 0.22 and $0.26^{\circ}\text{C dec}^{-1}$ over the USA due to $\Delta CC/\Delta t$.

Angell (1999) determined the zonal trends in surface and atmospheric temperatures over North America between 1973 and 1994. For comparison with the trends estimated here from the cirrus data, the average temperature trends for the surface and the troposphere between 850 and 300 hPa were taken from the layer means in Figs. 3 and 4 of Angell (1999) for the zones: 40-50°N, 30-40°N, and 20-30°N. The trends for the southernmost zone were given a weight of only 0.5 because the boundaries of the contiguous USA are north of 25°N. The computed mean annual and seasonal trends

(Table 4) are within 10-30% of the corresponding observations from Angell (1999). The USA seasonal ΔT_a trends are opposite those for the entire Northern Hemisphere where the weakest increases in temperature occur during winter and early spring, and the mean annual hemispheric trends are less than half those over the USA (Pielke et al. 1998). These results demonstrate that the increased cirrus coverage, attributed to air traffic, could account for nearly all of the surface and tropospheric warming observed over the USA between 1975 and 1994.

5. Concluding remarks

The estimated temperature changes are based on a simple application of limited GCM calculations and assume that cirrus coverage is the only parameter changing during the period. Other GCM formulations may yield different results than that used here. Changes in aerosol concentrations, greenhouse gases, and the geographical distribution of clouds, as well as other air traffic effects, were not taken into account. For example, ozone formed from air traffic exhaust is expected to produce a positive radiative forcing comparable to that from contrails and would result in additional tropospheric warming below the flight levels (IPCC, 1999). Also, contrails that form in existing cirrus clouds and do not contribute additional cirrus cloud cover can increase the cirrus optical depth further affecting $FNET$. Despite the good correlations between $RH3$ and CC outside of heavy-air-traffic land areas, UTH estimates must be viewed with some skepticism because filtering of observations may have eliminated significant portions of the soundings available for assimilation by NCEP. Better measurements of UTH, cloud distributions, and contrail properties and more precise specification of flight paths and

improved parameterizations of cirrus and contrail formation in GCMs are needed to more rigorously determine the contrail climate impacts. This study indicates that contrails already have substantial regional effects where air traffic is heavy. As air travel continues growing in other areas, the impact may become globally significant.

REFERENCES

- Angell, J. K., 1999: Variation with height and latitude of radiosonde temperature trends in North America, 1975-94. *J. Climate* **12**, 2551-2561.
- Bates, J. J. and D. L. Jackson, 2001: Trends in upper-tropospheric humidity. *Geophys. Res. Lett.* **28**, 1695-1698.
- Boucher, O., 1999: Air traffic may increase cirrus cloudiness. *Nature*, **397**, 30-31.
- Changnon, S. A., 1981: Midwestern cloud, sunshine and temperature trends since 1901: Possible evidence of jet contrail effects. *J. Appl. Meteorol.* **20**, 496-508.
- Duda, D. P., P. Minnis, and L. Nguyen, 2001: Estimates of cloud radiative forcing in contrail clusters using GOES imagery. *J. Geophys. Res.*, **106**, 4927-4937.
- Duda, D. P., P. Minnis, L. Nguyen, and R. Palikonda, 2003: A case study of contrail evolution over the Great Lakes. Submitted *J. Atmos. Sci.* Available at <http://www-pm.larc.nasa.gov/sass/pub/journals/jas.duda.2003.pdf>
- European Center for Medium Range Forecasting. *ECMWF 1995. The Description of the ECMWF/WCRP Level III-A Global Atmospheric Data Archive.* (Available at <http://www.ecmwf.int/products/data/archive/descriptions/od/toga/>)
- Elliot, W. P. and D. J. Gaffen, 1991: On the utility of radiosonde humidity archives for climate studies. *Bull. Amer. Meteor. Soc.* **72**, 1507-1520.
- Elliot, W. P., R. J. Ross, W. H. Blackmore, 2002: Recent changes in NMW upper-air observations with emphasis on changes from VIZ to Vaisala radiosondes. *Bull. Amer. Meteor. Soc.*, **83**, 1003-1017.
- Elliot, W. P., R. J. Ross, and B. Schwartz, 1998: Effects on climate records of changes in National Weather Service humidity processing procedures. *J. Climate*, **11**, 2424-2436.

- Eskridge, R. E., O. A. Alduchov, I. V. Chernykh, P. Zhai, A. C. Polansky, and S. R. Doty, 1995: A Comprehensive Aerological Reference Dataset (CARDS): Rough and systematic errors. *Bull. Amer. Meteor. Soc.* **76**, 1759-1775.
- Gaffen, D. J., 1993: *Historical Changes in Radiosonde Instruments and Practices*. WMO/TD-No. 541.
- Gierens, K., U. Schumann, M. Helten, H. Smit, and A. Marenco, 1999: A distribution law for relative humidity in the upper troposphere and lower stratosphere derived from three years of MOZAIC measurements. *Ann. Geophysicae* **17**, 1218-1226.
- Hahn, C. J. and S. G. Warren, S.G., 1999: *Extended Edited Synoptic Cloud Reports from Ships and Land Stations Over the Globe, 1952-1996*. NDP026C, Carbon Dioxide Information Analysis Center, Oak Ridge National Laboratory, OAK Ridge, TN)
- Hansen, J., M. Sato, and R. Ruedy, 1997: Radiative forcing and climate response. *J. Geophys. Res.* **102**, 6,831-6,864.
- Intergovernmental Panel on Climate Change, 1999: *Special Report: Aviation and the Global Atmosphere*. Cambridge Univ. Press,
- Jensen, E. *et al.*, 2001: Prevalence of ice-supersaturated regions in the upper troposphere: Implications for optically thin ice cloud formation. *J. Geophys. Res.* **106**, 17,253-17,266.
- Jensen E. and O. Toon, 1994: Ice nucleation in upper troposphere: Sensitivity to aerosol number density, temperature, and cooling rate. *Geophys. Res. Lett.* **21**, 2019-2022.
- Kistler, R. *et al.*, 2001: The NCEP-NCAR 50-year reanalysis: Monthly means CD-ROM and documentation. *Bull. Amer. Meteor. Soc.* **82**, 247-267.

- Marquart, S. and B. Mayer, 2002: Towards a reliable GCM estimation of contrail radiative forcing. *Geophys. Res. Lett.*, **29**, 10.1029/2001GL014075.
- Meerkötter, R. U. Schumann, D. R. Doelling, P. Minnis, T. Nakajima and Y. Tsushima, 1999: Radiative forcing by contrails. *Ann. Geophysicae* **17**, 1070-1084.
- Meyer, R., H. Mannstein, R. Meerkötter, U. Schumann, and P. Wendling, 2002: Regional radiative forcing by line-shaped contrails derived from satellite data. *J. Geophys. Res.* **107**, D10 10.1029/2001JD000426.
- Miloshevich, L. M., H. Vömel, A. Paukkunen, A. J. Heymsfield, and S. J. Oltmans, 2001: Characterization and correction of relative humidity measurements from Vaisala RS80-A radiosondes at cold temperatures. *J. Atmos. Oceanic Technol.* **18**, 135-156.
- Minnis, P., J. K. Ayers, S. P. Weaver, and M. L. Nordeen, 2003: Contrail frequency over the USA from surface observations. *J. Climate*, in press.
- Minnis, P., L. Nguyen, D. P. Duda, and R. Palikonda, 2002: Spreading of isolated contrails during the 2001 air traffic shutdown. *Proc. Amer. Meteor. Soc. 10th Conf. Aviation, Range, Aerospace Meteorol.*, Portland, OR, May 13-16, J9-J12.
- Minnis, P., D. F. Young, L. Nguyen, D. P. Garber, W. L. Smith Jr., and R. Palikonda, 1998: Transformation of contrails into cirrus during SUCCESS. *Geophys. Res. Lett.* **25**, 1157-1160.
- Minnis, P., U. Schumann, D. R. Doelling, K. Gierens, and D. Fahey, 1999: Global distribution of contrail radiative forcing. *Geophys. Res. Lett.* **26**, 1853-1856.
- Nakanishi, S., J. Curtis, J. and G. Wendler, 2001: The influence of increased jet airline traffic on the amount of high level cloudiness in Alaska. *Theor. Appl. Climatol.* **68**, 197-205.

- Palikonda, R., P. Minnis, P. K. Costulis, and D. P. Duda, 2002: Contrail climatology over the USA from MODIS and AVHRR data. *Proc. Amer. Meteor. Soc. 10th Conf. Aviation, Range, Aerospace Meteorol.*, Portland, OR, May 13-16, J9-J12.
- Palikonda, R., P. Minnis, D. R. Doelling, P. W. Heck, D. P. Duda, H. Mannstein, and U. Schumann, 1999: Contrail climatology over the USA from MODIS and AVHRR data. *Proc. Amer. Meteor. Soc. 10th Conf. Atmos. Rad.*, Madison, WI, 28 June – 2 July, 181-184.
- Pielke, R. A., J. Eastman, T. N. Chase, J. Knaff, and T. G. F. Kittel, 1998: 1973-1996 trends in depth-averaged tropospheric temperature. *J. Geophys. Res.* **103**, 16,927-16,933.
- Ponater, M., S. Marquart, and R. Sausen, 2002: Contrails in comprehensive global climate model: parameterisation and radiative forcing results. *J. Geophys. Res.* **107**, 10.1029/2001JD000429.
- Rind, D., P. Lonergan, and K. Shah, 2000: Modeled impact of cirrus cloud increases along aircraft flight paths. *J. Geophys. Res.* **105**, 19,927-19,940.
- Rossow, W. B. and R. A. Schiffer, 1999: Advances in understanding clouds from ISCCP. *Bull. Amer. Meteor. Soc.* **80**, 2261-2287.
- Sassen, K., 1997: Contrail-cirrus and their potential for regional climate change. *Bull. Amer. Meteor. Soc.* **78**, 1885 –1903.
- Sassen, K. and G. C. Dodd, 1989: Haze particle nucleation simulations in cirrus clouds, and application for numerical and lidar studies. *J. Atmos. Sci.* **46**, 3005-3014.

- Sausen, R., K. Gierens, M. Ponater, M. and U. Schumann, 1998: A diagnostic study of the global coverage by contrails, part I, present day climate. *Theor. Appl. Climatol.* **61**, 127-141.
- Soden, B. J. and J. R. Lanzante, 1996: An assessment of satellite and radiosonde climatologies of upper-tropospheric water vapor. *J. Climate* **9**, 1235-1250.
- Travis, D., A. Carleton, and R. Lauritsen, 2002: Contrails reduce daily temperature range. *Nature*, **418**, 601.
- Warren, S. G., C. J. Hahn, J. London, R. M. Chervin, and R. L. Jenne, *National Center for Atmospheric Research Technical Note 273+STR*, (1986)
- Warren, S. G., C. J. Hahn, J. London, R. M. Chervin, and R. L. Jenne, *National Center for Atmospheric Research Technical Note 317+STR* (1988).
- Udelhofen, P. and R. D. Cess, 2001: Cloud cover variations over the United States: An influence of cosmic rays or solar variability. *Geophys. Res. Lett.*, **28**, 2617-2620.

Acknowledgements

Many thanks to D. Young and D. Duda for critical reviews, U. Schumann and D. Fahey for their comments, K. Gierens for providing the contrail distributions, C. Hahn for assistance with the cirrus data, D. Doelling for assistance in analyzing the radiosonde data, and D. Minnis for continued encouragement. This research was supported by the NASA Office of Earth Science Pathfinder Program under NRA-99-OES-04.

Table 1. Boundaries of the air traffic regions. LOR and OOR do not include any of the areas within the remaining land and ocean ATRs.

ATR	Latitude	Longitude
Asia	35°N – 70°N	90°E – 180°E
EUR	35°N – 70°N	30°W – 40°E
WEUR	40°N – 60°N	10°W – 15°E
USA	25°N – 50°N	60°W – 130°W
LOR	70°S – 70°N	180°W – 180°E
NA	35°N – 70°N	70°W – 20°E
NP	35°N – 70°N	120°E – 110°W
OOR	70°S – 70°N	180°W – 180°E

Table 2. Contrails, mean cirrus cover, and cloudiness trends (%/decade) over ATR regions from surface and ISCCP data. The numbers in parentheses indicate the interannual variability in *CC*. The 1971-95 trends in *CC* are all significant at the 99% confidence level, except over WEUR where no trend is apparent.

Region	1992 <i>ECON</i> (%)	Mean <i>CC</i> (%) 1971-95	<i>CC</i> Trend 1971-95	Total Cloud Trend 1971-95	<i>CC</i> Trend, 1983-95	ISCCP Trend, 1983-95
Western Asia	0.08	36.2 (1.0)	-0.9	-0.7	-2.0	-2.1
EUR	0.60	18.5 (1.3)	-1.2	-0.4	-0.4	0.0
WEUR	1.52	19.8 (1.4)	0.0	-0.7	1.8	0.9
USA	1.75	29.2 (1.1)	1.0	0.5	0.3	2.3
Land OR	0.09	24.5 (0.5)	-1.6	-1.4	-1.5	-0.6
North Atlantic	0.32	15.3 (0.7)	0.7	0.0	0.3	0.2
North Pacific	0.16	15.7 (0.8)	0.9	0.8	1.6	-0.4
Ocean OR	0.13	14.4 (0.6)	0.7	1.2	0.8	0.1

Table 3. Trends in mean 300-hPA relative humidity from NCEP, 1971-1995.

ATR	Trend in $RH3$, %/dec	Mean Temperature (K)
Asia	-3.2	223.1
EUR	-5.0	225.7
WEUR	-6.2	226.7
USA	-0.2	230.5
LOR	-1.2	230.4
NA	-1.8	227.6
NP	-1.7	230.0
OOR	-1.3	235.4

Table 4. Tropospheric and surface temperature trends, $\Delta T_a/\Delta t$, in °C/dec computed using the observed cirrus trends over the USA and from radiosonde data over North America between 20°N and 50°N from Angell (1999). The trends are generally consistent with the seasonal variation of contrail coverage in Fig. 4.

	Cirrus	Radiosonde
	$\Delta T_a/\Delta t$ (3-10 km)	$\Delta T_a/\Delta t$ (850-300 hPa)
	$[\Delta T_a/\Delta t]$ (surface)	$[\Delta T_a/\Delta t]$ (surface)
Winter	0.34 [0.29]	0.46 [0.43]
Spring	0.36 [0.31]	0.32 [0.38]
Summer	0.18 [0.15]	0.17 [0.15]
Fall	0.17 [0.14]	0.19 [0.13]
Annual	0.26 [0.22]	0.29 [0.27]

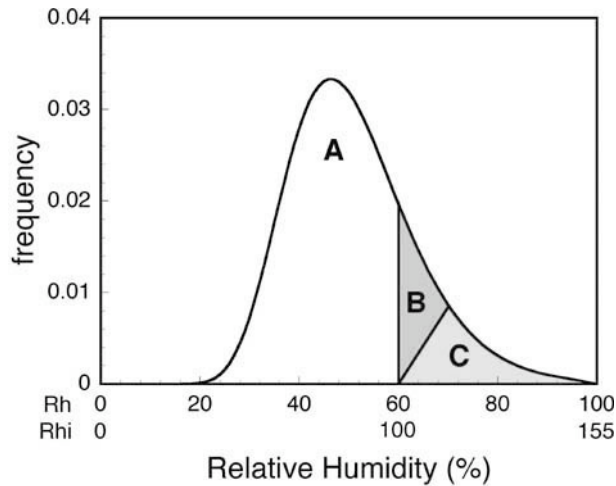


Fig. 1. Hypothetical annual relative humidity probability distribution at flight altitudes with $T = -50^{\circ}\text{C}$. Neither persistent contrails nor cirrus clouds would occur for $Rhi < 100\%$ (area A). Cirrus clouds and persistent contrails can form when $Rhi > 100\%$, but the probability of forming cirrus through natural nucleation processes increases as humidity rises (area C) leaving the potential for development of additional cirrus coverage from contrails (area B) via nucleation from mixing of moist jet engine exhaust with ice-saturated ambient air. The portion of area B that is converted from clear air to cloudy air should rise as the cumulative flight path length increases over a given area with growing air traffic. Areas B and C correspond to Rh between 60 and 100%.

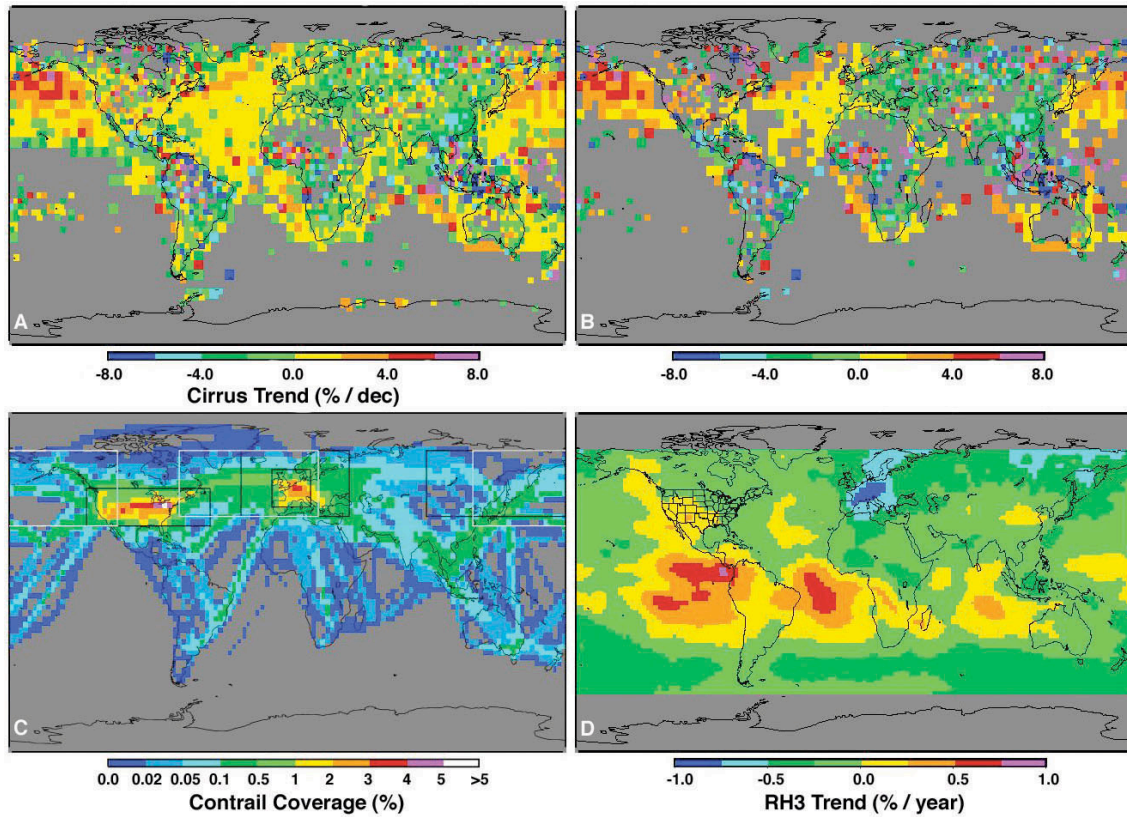


Fig. 2. Trends in cirrus coverage and 300-hPa relative humidity (1971-1995) and estimated 1992 linear contrail coverage. (a) Trends in cirrus coverage for all regions with more than 15 years of data. (b) Subset of (a) for all regions having trends significant at the 90% confidence level according to Student-t test. (c) Estimated linear contrail coverage. Black and white boxes determine the boundaries for the land and ocean ATRs, respectively. Only observations taken from land stations and from ships are used for the land and ocean ATRs, respectively. (d) Trends in annual mean NCEP relative humidity at 300 hPa.

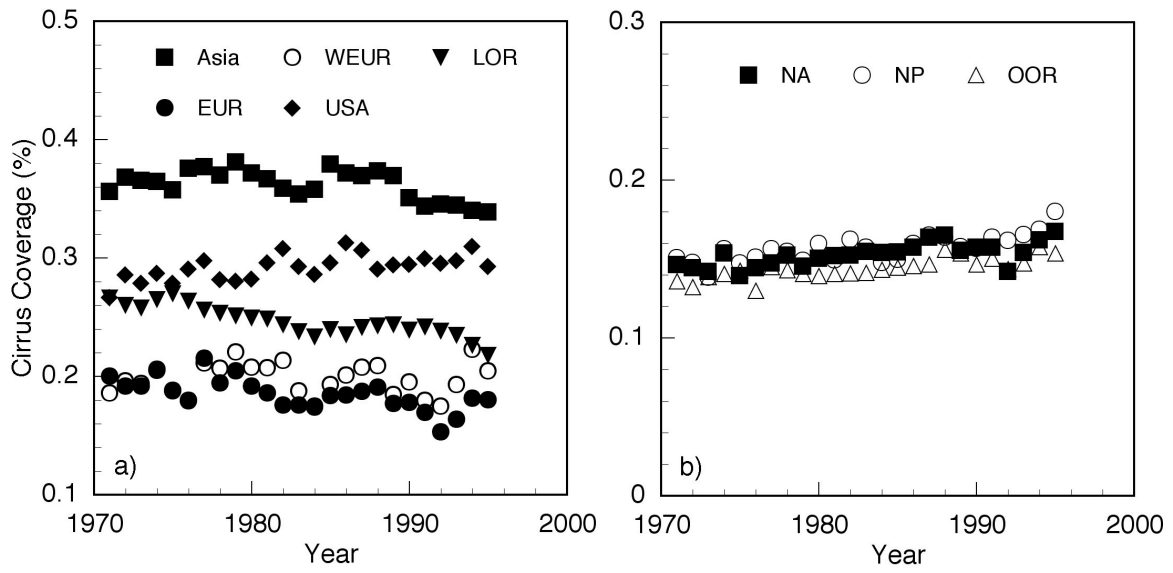


Fig. 3. Annual variation of CC over (a) land and (b) ocean.

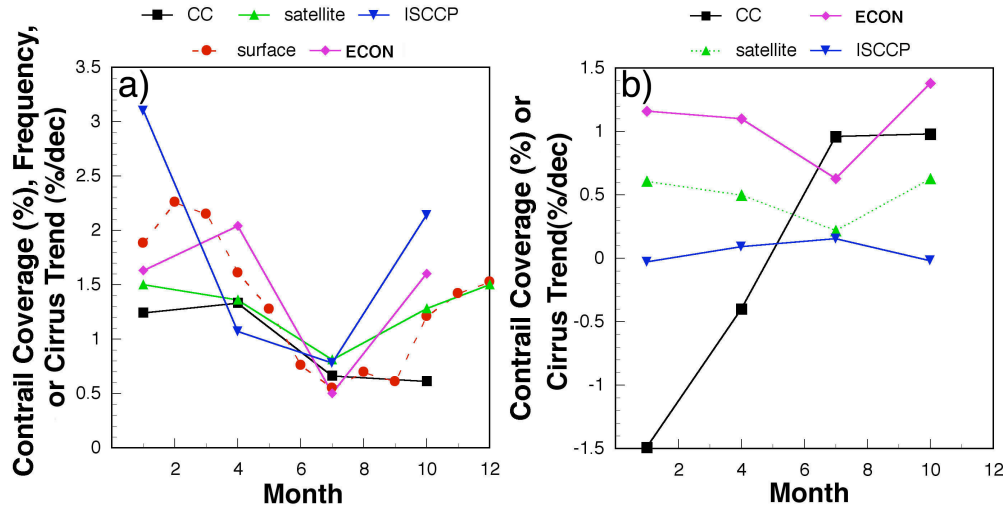


Fig. 4. Seasonal trends in cirrus and contrail amounts and frequencies over (a) the USA and (b) WEUR. The ISCCP and *CC* lines are cirrus trends. The *ECON* lines correspond to expected contrail coverage for 1992. Satellite denotes mean linear contrail coverage derived from satellite data during the mid-1990's. Surface data denote persistent contrail frequency observed from the surface during the 1990's. The USA winter and spring trends are significant at the 99% confidence level compared to 84% for summer and fall. Only the summer *CC* trend over WEUR is significant at the 99% confidence level, while the winter and fall trends are significant at the 84% confidence level. The WEUR spring trend is not statistically significant. If cirrus coverage is increasing because of contrail generation, then it should increase proportionately with contrail coverage. This idea is borne out by data over the USA, but not over WEUR.

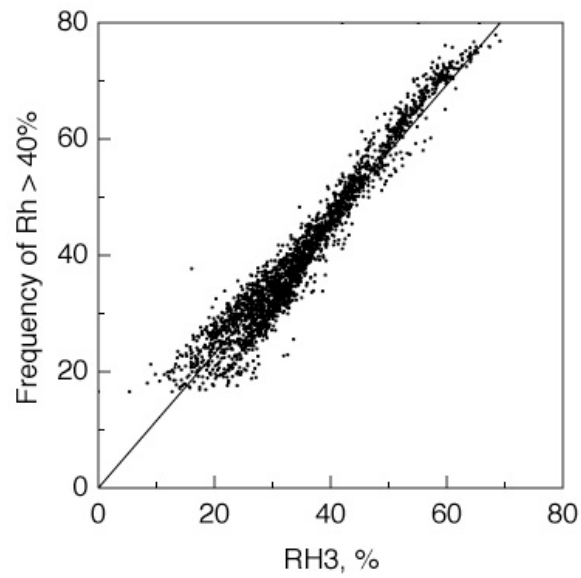


Fig. 5. Variation of the frequency of occurrence of $Rh(300 \text{ hPa}) > 40\%$ with $RH3$ from CARDS rawinsonde data from 77 stations, 1971-2000. Contrail formation and cirrus persistence are highly probable if $Rh(300 \text{ hPa}) > 40\%$. Thus, $RH3$ can serve as a predictor for cirrus persistence.

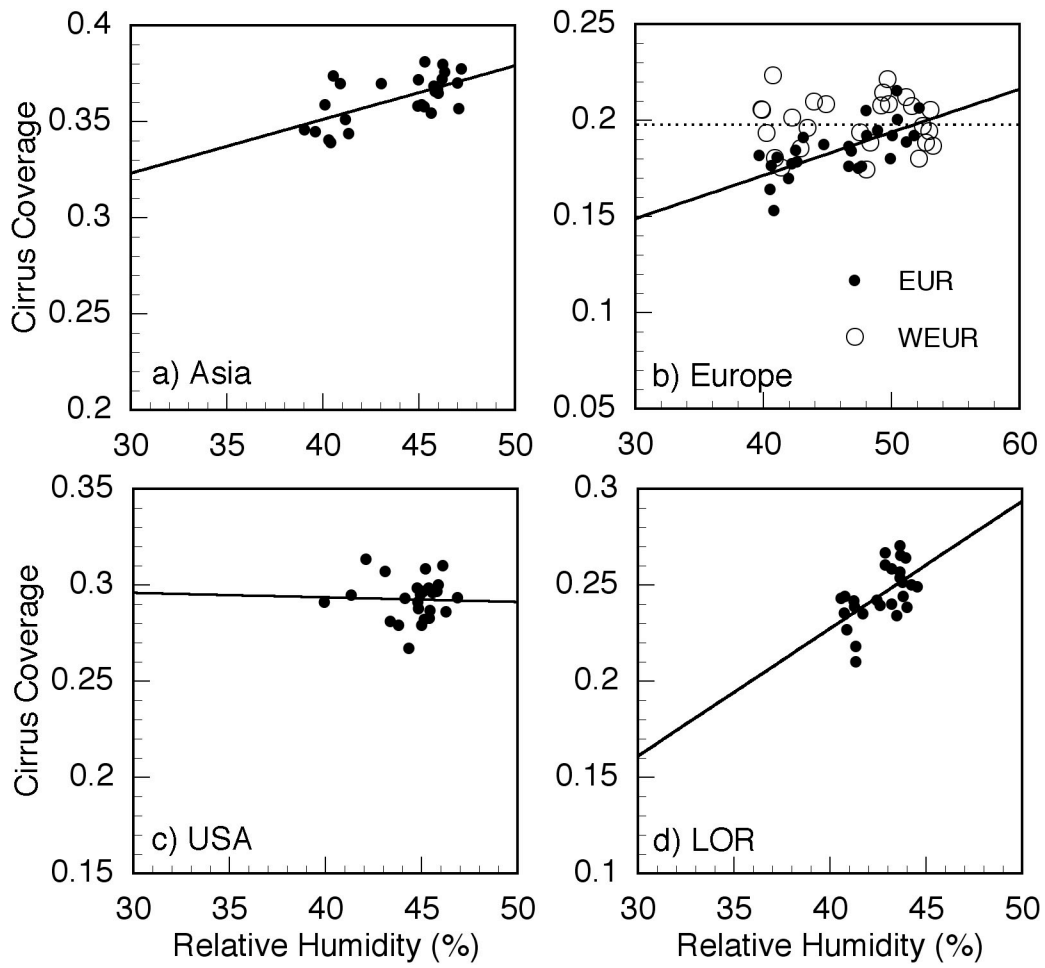


Fig. 6. Correlation of $RH3$ and mean annual CC , 1971-1995.

Appendix

When compared with satellite estimates of UTH, radiosonde measurements of Rh are overestimated for the former Soviet Union and China and underestimated over the USA and western Europe (Soden and Lanznte, 1996). The satellite-radiosonde discrepancies were attributed to the use of different types of humidity instruments. Relative to the CARDS values, the NCEP re-analyses reduced $RH3$ over Asia (Fig. A1a) and increased $RH3$ over Europe (Fig. A1b) and the USA (Fig. A1c). Over other parts of the globe, $RH3$ increased by $\sim 15\%$ compared to the CARDS values (Fig. A1d). The NCEP trends are consistent with the CARDS data over Europe and the rest of the globe. Over the USA, the CARDS data show a rise in $RH3$ with year, while the NCEP $RH3$ shows no significant trend. The USA CARDS $RH3$ values are probably the least reliable of considered datasets, however, because only 65% of the 104,419 soundings taken between 1971 and 2000 that had a valid Rh at 400 hPa also had a valid Rh at 300 hPa. Furthermore, only 25% of the 400-hPa-valid soundings had a valid Rh when $T < 233\text{K}$. Prior to October 1993, Rh was not reported for $T < 233\text{K}$ and it was set equal to 19% whenever the measured value was less than 20% (Elliot et al. 1998). Most of the valid cold Rh values occurred after 1993 when reporting practices began to include Rh at all levels regardless of temperature (Elliot et al. 2002). A variety of other problems plague the USA radiosonde record (Eskridge et al. 1995; Elliot et al. 1998, 2002). Since the NCEP reanalysis adjusts values to achieve model consistency and computes $Rh(300\text{ hPa})$ for all temperatures, it is not surprising that the NCEP and CARDS $RH3$ trends are different. Valid $Rh(300\text{ hPa})$ values occurred 84%, 77%, and 77% of the time over Asia, Europe,

and the rest of globe, respectively, in the CARDS data when $T(300 \text{ hPa}) < 233\text{K}$ and $Rh(400 \text{ hPa})$ was valid.

The CARDS and NCEP $RH3$ values are well correlated over EUR, WEUR, and OOR, but not over western Asia over the USA (Fig. A2). Over Asia, $RH3$ from NCEP and CARDS diverge after 1986 resulting in the diminished correlation between NCEP and the CARDS $RH3$. Documentation of the radiosonde data taken over western Asia (Elliot and Gaffen, 1991) does not indicate any significant changes around 1986. However, the statistically significant decrease in CC over western Asia (Table 2) supports the negative trend in $RH3$ suggesting the possibility of some unreported changes in instrumentation or reporting practices in one or more reporting countries. The lack of correlation over the USA is not surprising because the CARDS profiles lack values for most of the cold seasons as discussed above.

The greatest values of CC occur over Western Asia suggesting that $RH3$ should be larger there than in any other ATR. Because the dry bias in the measurements depends on temperature, the measurements and, hence, the NCEP $RH3$ values would be lower than over other regions because the 300-hPa temperature (Table 2) is 7 K less than anywhere else. An empirical correction formula (Minnis et al. 2002) indicates that at 223K, the measured Rh would be nearly 21% less than true value at ice saturation compared to that at 230K, which would be only 14% less than the corresponding true value at ice saturation. If such biases hold for the NCEP data, then approximately 7% should be added to the $RH3$ values over Asia resulting in the Asian values exceeding their USA counterparts. Given the poor state of UTH measurements and their use in

assimilation models, it is not expected that the absolute value of $RH3$ will be highly accurate for a given region.

Trends in $RH3$ and in the average RH between 300 and 500 hPa were computed for 1979-1998 for comparison with satellite-derived values of UTH (Bates and Jackson, 2001). A comparison with Fig. 1 from Bates and Jackson (2001) indicates that the NCEP trends are generally opposite in sign to those from the satellite data over most land areas. Better agreement was found over the oceans. The trends in $RH3$ from NCEP were also compared to those from the European Center for Medium Range Forecasting (ECMWF) monthly TOGA Global Tropospheric Analyses for 1985-1996 (Fig. A3) when ECMWF data are available (ECMWF 1995). In general, the ECMWF trends are more extreme than their NCEP counterparts. They agree in sign over Europe, western Asia south of 50°N, and over much of the NP and NA. The trends are opposite in sign over many other areas including the USA and Australia. The NCEP trends are only significant at the 90% confidence level over the western USA, Europe, Siberia, China, and Australia. The ECMWF trends are significant over the eastern USA, Europe, China, southern Asia, Siberia, and Australia. Thus, the two datasets show some significant disagreement. Both datasets were correlated with CC for the various ATRs. The values of R^2 for the ECMWF $RH3$ were all less than 0.12 and none of the correlations were statistically significant.

The only UTH data available for 1971-96 are from CARDS or NCEP. ECMWF reanalyses are not yet available for the entire time period. Of all of the data available for any significant time period, only the NCEP $RH3$ values show significant correlations with CC for areas where contrails should play a minor role in cirrus coverage. The correlations over ocean are significant but of the wrong sign. Further study is needed to

understand this behavior over oceans. The CARDS data are available only over a limited number of sites and overall are not correlated with *CC* any better than the NCEP data. By default, the NCEP dataset is the only one available for comparison with the *CC* trends. From all of the available evidence, however, it appears that the NCEP data over land make the most sense and, therefore, are the most appropriate UTH dataset for the study period or any significant portion of it.

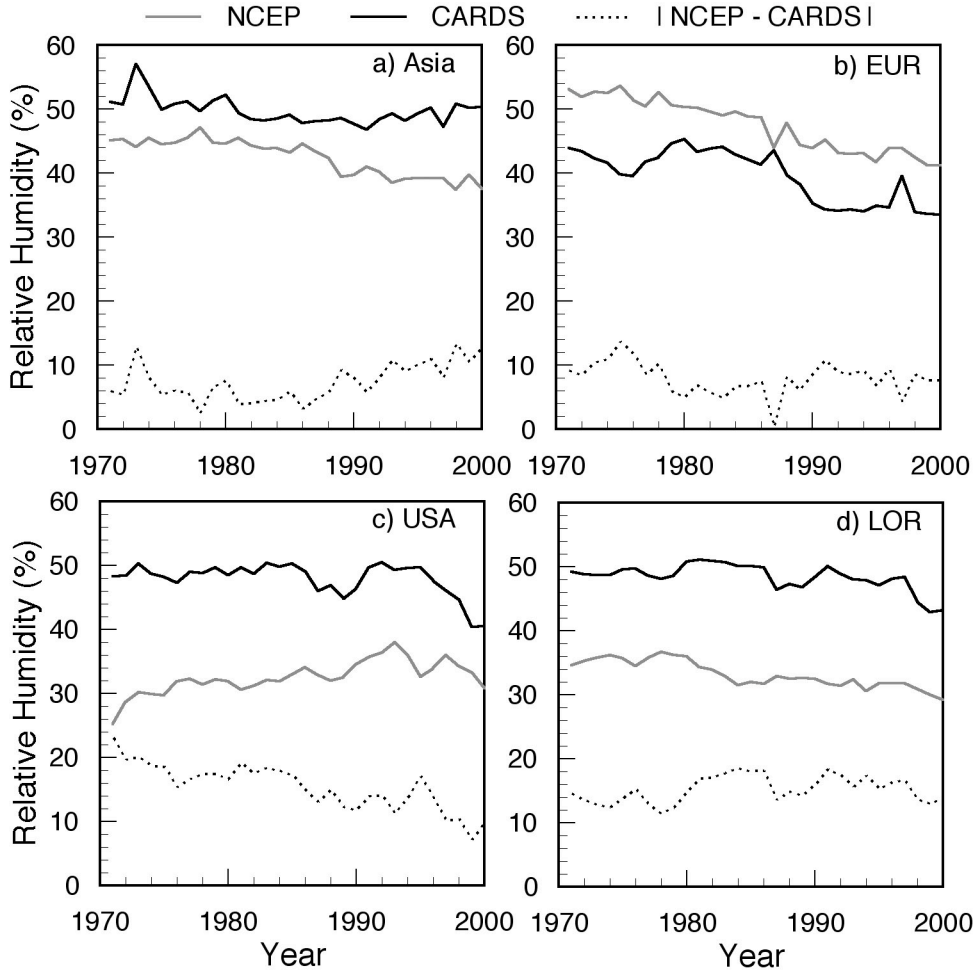


Fig. A1. Comparisons of annual mean 300-hPa relative humidities over CARDS sites within the ATRs. DIFF indicates the absolute value of the difference between the two estimates of $RH3$.

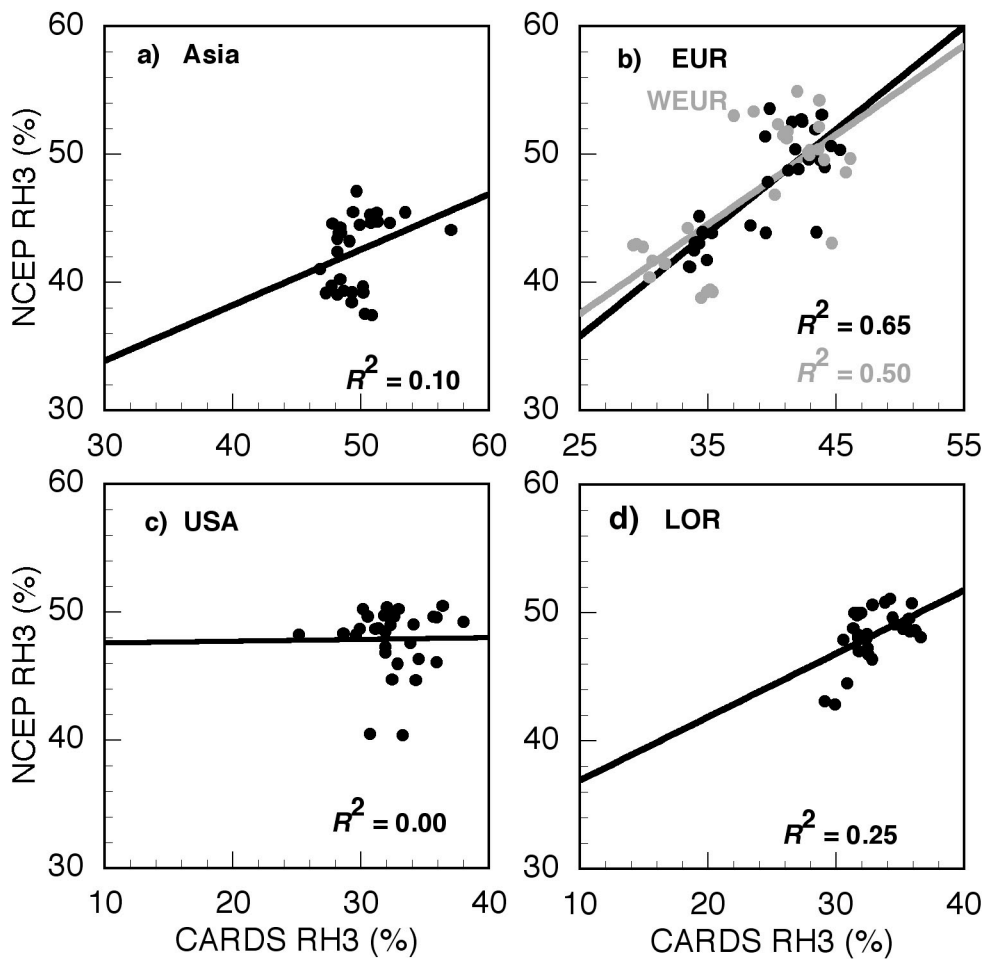


Fig. A2. Correlations of *RH3* data shown in Fig. A1.

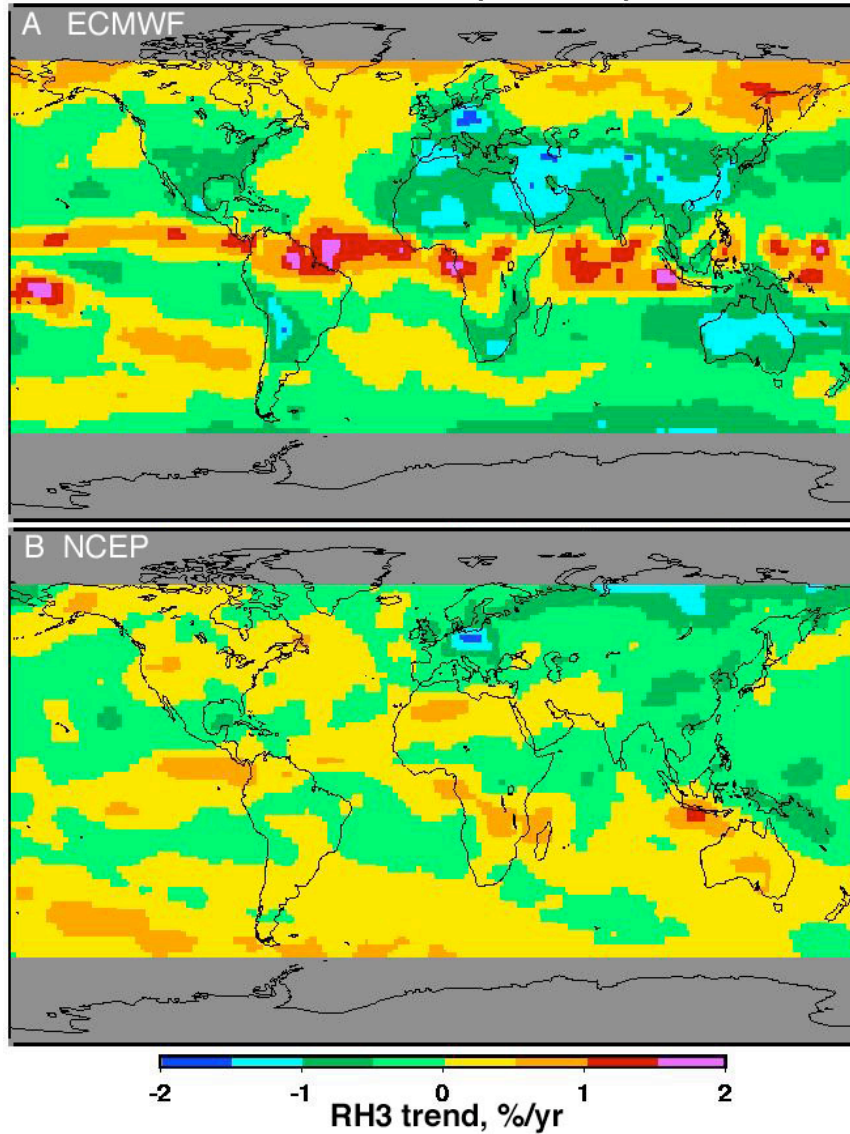


Fig. A3. 1985-1996 trends in $RH3$ from A) ECMWF and B) NCEP reanalyses.